Theory of Idealized Two-Dimensional Ballute in Newtonian Hypersonic Flow

Chul Park*
NASA Ames Research Center, Moffett Field, California

A differential equation governing the geometry of a two-dimensional ballute in hypersonic flow and its constraining boundary conditions are derived under idealized assumptions. By solving these equations, the shape of the ballute is determined over a range of conditions. Lift, drag, pitching moment, and the allowed limit of center-of-gravity location for stability (metacenter) are then calculated using Newtonian hypersonic approximation. It is shown that the metacenter occurs near the forward end because of compliance of the ballute membrane to the shock-layer pressures, especially at low freestream densities. In order for the vehicle employing the ballute to be stable at all densities, the center of gravity must be within approximately the forward 20% of the overall length of the vehicle. However, typical flight trajectories of an aeroassisted orbital transfer vehicle employing the ballute for aerobraking show that the vehicle may be able to complete its atmospheric flight without tumbling provided that the center of gravity is located within the forward 43% of the vehicle length, because of the relatively short duration of flight through the destabilizing low-density regime.

Nomenclature

A = area of the fuselage, m^2
c.g. = center of gravity
c.p. = center of pressure
C_d = drag coefficient
C_ℓ = lift coefficient
C_m = pitching moment coefficient
I = moment of inertia, kg-m^2
L_0 = length of fuselage (vehicle), m
L_a = distance from leading edge to c.p., m
L_b = distance from leading edge to metacenter, m
L_c = distance from leading edge to c.g., m
M = vehicle mass, kg
p = pressure, N/m^2
R = radius of curvature of base region, m
S_0 = unstretched length of ballute membrane, m
T = tension, N/m
U = freestream velocity, m/s
x,y = horizontal and vertical coordinates, normalized by R (see Fig. 2)
x',y' = horizontal and vertical coordinates, m (see Fig. 2)
Y_a = distance from centerline to c.p., m
Z = horizontal drift in flight trajectory, m (see Fig. 3)
α = angle of attack of vehicle, rad
β = trailing-edge interception angle, rad (see Fig. 2)
γ = bearing error in flight trajectory, rad (see Fig. 3)
Δ = overpressure parameter, dimensionless [see Eq. (4)]
ϵ = body angle, rad (see Fig. 3)
θ = local angle of attack, rad
ρ = freestream density, kg/m^3
σ = fractional elongation, dimensionless
ϕ = elastic constant of membrane, N/m
χ = pressure-to-elasticity ratio, dimensionless [see Eq. (16)]

Subscripts
a = center of pressure
b = metacenter (the farthest downstream c.g. location allowed)
c = center of gravity
ℓ = leading edge

Presented as Paper 86-0301 at the AIAA 24th Aerospace Sciences Meeting, Reno, NV, Jan. 6-9, 1986, Reno, NV; received April 2, 1987; revision received.

*Research Scientist. Associate Fellow AIAA.

Introduction

THE concept of aeroassisted orbital transfer vehicles (AOTV) has been developing rapidly in recent years.[1,2] A space-based AOTV is believed to be able to carry commercial satellites from a low Earth orbit to the geosynchronous Earth orbit (GEO) and return expending less fuel and more reliably than other alternative vehicles (such as an expendable rocket vehicle or an orbital transfer vehicle without aeroassist). This advantage is gained by flying through the upper atmosphere of the Earth on return from GEO, thereby reducing the vehicle velocity by air drag, rather than by expending fuel in retrorocket burn.

Several design schemes have been proposed for the aerobrake. One of these proposed designs uses a ballute, which is an elastic bag inflated with internal gas pressure.[3-5] According to the proposal, the rocket engines may be placed either at the forward or aft end of the ballute. When the engines are placed at the forward end, drag of the system can be modulated by bleeding a small amount of fuel (without burning), and thus varying the flowfield around the ballute. When the engines are placed at the aft end, drag must be controlled by varying the internal gas pressure, which, in turn, varies the shape and size of the ballute. In the upper part of Fig. 1, such a vehicle is schematically illustrated with an engine located at the aft end of the ballute. The main body of the vehicle, which contains fuel tanks, payload, and guidance and control systems, will be called fuselage in the present work, as indicated in the figure. The meridian tapes shown in the figure must be elastic for the case when the rocket engine is located at the aft end, and they must bear most of the forces generated by the ballute membrane and transmit them to the fuselage.

The general concept of a ballute for use as a means of decelerating aerospace vehicles and objects has been studied by various investigators since the late 1960's.[6-13] To the author's knowledge, in all such studies the ballute is placed behind the vehicle or the object, i.e., in a towing position. The ballute is mechanically connected to the main vehicle by a towing cable, and the drag force produced by the ballute is

transmitted to the vehicle through a swivel placed at the forward end of the ballute: the ballute is free to rotate around the swivel in all directions. Flight and wind-tunnel tests at subsonic, supersonic, and low hypersonic speeds[8-10,13] demonstrated that the ballute in this position develops a small oscillatory (tail-wagging) motion around the swivel, but since its amplitude does not diverge, the motion can be considered aerodynamically stable. That is, the ballute is conditionally stable around the forward-end point (leading edge).

In the proposed application for AOTV's, however, a ballute is not in the towing position. Instead, it surrounds the fuselage of the vehicle as shown in the upper part of Fig. 1. In order for the system to be aerodynamically stable in this configuration the first derivative of the pitching moment around the c.g. with respect to the angle of attack must be negative. The c.g. is located, in general, between the forward and aft ends of the fuselage. Alternatively, a vehicle is absolutely stable if the c.p. is located behind the c.g. (this is a sufficient condition but not a necessary condition). Nothing is known presently about the pitching moment characteristics or the location of c.p. for ballutes at the hypersonic Mach numbers expected of an AOTV. During a typical expected mission of an AOTV, the c.g. will shift considerably as the vehicle loads or unloads its payload or as fuel is consumed. The vehicle should be designed to maintain stability with any resulting c.g. location.

To determine the pitching moment of a ballute at a given angle of attack, one must first know the shape of the ballute at the angle of attack. To determine the shape theoretically, one must first derive equations governing the geometry. The mechanics governing a realistic, axisymmetric ballute are complicated and virtually beyond our comprehension at present. In order to satisfy the urgent need to know the approximate ballute characteristics and to provide the guidance needed for analyzing the axisymmetric case, the present work proposes a two-dimensional idealized ballute concept, as shown in the lower part of Fig. 1. It is believed that the knowledge gained about such a two-dimensional body is applicable, at least qualitatively, to an axisymmetric case. In this idealized ballute, the fuselage is assumed to be compressed to zero thickness as shown. This assumption should be almost valid, since the frontal area of the fuselage is small when compared with that of the ballute. Analysis of this ballute is much simpler than the axisymmetric ballute, as will become apparent. Other assumptions used are:

1) The ballute membrane has no mass: the entire mass of the vehicle is possessed by the infinitesimally thin fuselage.

2) The ballute membrane is a perfect elastomer (tension proportional to elongation) of uniform elastic coefficient and thickness.

3) The airflow around the vehicle can be described by Newtonian hypersonic theory with zero friction.

4) The internal presure is the same in both the upper and lower compartments.

Assumptions 1, 2, and 4 are self-evident; they are reasonable approximations to the complex, real situations. Assumption 3, Newtonian approximation, was made here for simplicity. The Newtonian approximation is known to be inaccurate in comparison with other more elaborate methods. The extent of possible error due to this assumption can be estimated from Fig. 10 of Ref. 14, which compares Newtonian pitching moments with those obtained using a more accurate analytical method (HALIS) and with three sets of wind-tunnel data, for an AOTV configuration. According to the figure, the Newtonian method yields a trim angle of attack that is an approximate average of those obtained by the four other methods. The difference in the trim angle of attack between the Newtonian and HALIS methods is about 2 deg. This represents a difference in pitching moment coefficient of 0.008, or, equivalently, a discrepancy in c.p. location of 0.8% of the reference length, between the two methods.

Using these assumptions, the present work derives the equations governing the shape of the ballute membrane. By

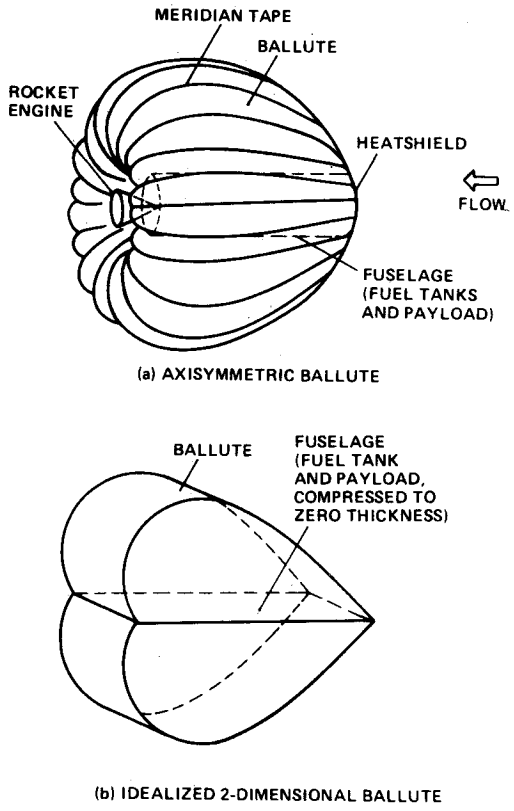

Fig. 1 Origin of the idealized two-dimensional ballute concept.

solving the equations and by integrating aerodynamic forces on the membrane surface over the shape so obtained, lift, drag, moment, and the allowed limit of c.g. location (metacenter) are determined. The results show that the metacenter of the vehicle is located relatively close to the forward-end (leading-edge) point. An explanation for this behavior is advanced. A flight trajectory calculation is performed for a hypothetical AOTV employing such a two-dimensional ballute for aerobraking purposes to demonstrate the consequence of this behavior. In addition, the analysis deduces the parameters that control the ballute geometry and, hence, aerodynamic characteristics. Knowledge of such parameters should be helpful in studying an axisymmetric ballute in the future.

Method of Calculation

The fundamental equation governing the geometry of a two-dimensional elastic membrane separating two regions of differing pressures can be derived by equating the forces acting across the membrane, leading to

$$\text{Curvature} \times \text{tension} = \text{pressure difference} \qquad (1)$$

Expressed in a Cartesian coordinate system using x' and y', and denoting curvature in terms of the first and second derivatives, dy'/dx' and d^2y'/dx'^2, tension by T, and pressure difference by Δp, Eq. (1) becomes

$$\frac{d^2y'}{dx'^2} - \frac{\Delta p}{T}\left[1 + \left(\frac{dy'}{dx'}\right)^2\right]^{1.5} = 0 \qquad (2)$$

The coordinates x' and y' chosen for the present analysis are illustrated in Fig. 2: the x' axis is parallel to the freestream flow, and the origin is at the shoulder (the border between the forebody and the base). Only one (lower) of the two (upper and lower) compartments of the ballute is analyzed at a time

as shown. The quantity Δp is the difference between the internal and external pressures

$$\Delta p = \text{Internal pressure} - \text{external pressure} \tag{3}$$

For the sake of convenience, the internal pressure will be expressed in the present work by

$$\text{Internal pressure} = (1 + \Delta)\rho U^2 \tag{4}$$

The quantity Δ is a measure of how much higher the internal pressure is in comparison with the total pressure of the freestream flow and will be termed here overpressure parameter. It can theoretically vary from -1 to ∞, provided that other contraints permit. Under the assumption of a Newtonian hypersonic flow, the external pressure at any given point x', y' becomes

$$\text{External pressure} = \rho U^2\left(\frac{dy'}{dx'}\right)^2\Big/\left[1 + \left(\frac{dy'}{dx'}\right)^2\right] \tag{5}$$

In the domain left of the origin, i.e., in the base region, the external pressure becomes zero under the Newtonian assumption. Since both the internal pressure and tension force remain constant at every point on the ballute membrane, Eq. (1) dictates that curvature be constant in this domain. The radius of curvature in this domain will be designated by R.

Under the assumption of a perfect elastomer, tension T is expressible as

$$T = \sigma\phi \tag{6}$$

where σ and ϕ represent, respectively, the fractional elongation (dimensionless) and elastic constant (in units of Newtons per meter) for the tension force corresponding to the elongation. By substituting Eqs. (3-6) into Eq. (2), and normalizing x' and y' by

$$x = x'/R, \quad y = y'/R$$

one obtains the differential equation governing the shape of the ballute in the form

$$\frac{d^2y}{dx^2} - \left[1 - \left(\frac{1}{1+\Delta}\right)\left(\frac{dy}{dx}\right)^2\Big/\left\{1 + \left(\frac{dy}{dx}\right)^2\right\}\right]\left[1 + \left(\frac{dy}{dx}\right)^2\right]^{1.5} = 0 \tag{7}$$

Denoting the leading-edge point by subscript ℓ, drag and lift per unit width of the membrane (produced by one compartment) become

$$\text{Drag} = \rho U^2 R\int_o^\ell\left[\left(\frac{dy}{dx}\right)^3\Big/\left\{1 + \left(\frac{dy}{dx}\right)^2\right\}\right]dx \tag{8}$$

$$\text{Lift} = \rho U^2 R\int_o^\ell\left[\left(\frac{dy}{dx}\right)^2\Big/\left\{1 + \left(\frac{dy}{dx}\right)^2\right\}\right]dx \tag{9}$$

The pitching moments around the origin produced by lift and drag become

$$\text{Lift moment} = \rho U^2 R^2\int_o^\ell\left[x\left(\frac{dy}{dx}\right)^2\Big/\left\{1 + \left(\frac{dy}{dx}\right)^2\right\}\right]dx \tag{10}$$

$$\text{Drag moment} = \rho U^2 R^2\int_o^\ell\left[y\left(\frac{dy}{dx}\right)^3\Big/\left\{1 + \left(\frac{dy}{dx}\right)^2\right\}\right]dx \tag{11}$$

where ρ and U are freestream density and velocity, respectively.

The boundary conditions to the differential equation (7) are obtained from the requirements that 1) the two components (vertical and horizontal) of forces balance; namely, that the lift and drag forces that are generated on the ballute surface by the Newtonian hypersonic pressure forces equal the sum of all the vertical and horizontal forces acting on the fuselage, respectively; and 2) that the total length of the membrane is compatible with the elastic relationship, Eq. (6). The forces acting on the fuselage consist of the tension T exerted by the ballute membrane at the leading and trailing edges of the fuselage and the pressure force acting normal to the fuselage (Fig. 2). The drag balance relationship leads to

$$\frac{1}{1+\Delta}\int_o^\ell\left[\left(\frac{dy}{dx}\right)^3\Big/\left\{1 + \left(\frac{dy}{dx}\right)^2\right\}\right]dx = 1\Big/\sqrt{1 + (dy/dx)_\ell^2} + \cos\beta + \frac{L_0}{R}\sin\alpha \tag{12}$$

The lift balance relation becomes

$$\frac{1}{1+\Delta}\int_o^\ell\left[\left(\frac{dy}{dx}\right)^2\Big/\left\{1 + \left(\frac{dy}{dx}\right)^2\right\}\right]dx = -\left(\frac{dy}{dx}\right)^2\Big/\sqrt{1 + (dy/dx)_\ell^2} - \sin\beta + \frac{L_0}{R}\cos\alpha \tag{13}$$

where β is the angle of interception between the body centerline (fuselage) and the membrane at the trailing edge (Fig. 2). Denoting the unstretched length of the membrane by S_o, the normalized total length of the membrane becomes

$$(\pi - \beta) + \int_o^\ell\sqrt{1 + (dy/dx)^2}dx = (1 + \sigma)\frac{S_0}{R} \tag{14}$$

The second boundary condition (that the total length of membrane be consistent with the elastic relationship) is obtained by substituting the relationship for σ

$$\sigma = \frac{T}{\phi} = \frac{R}{\phi}\rho U^2(1 + \Delta)$$

into Eq. (14), leading to

$$\left[1 + \frac{R}{\phi}\rho U^2(1 + \Delta)\right]\frac{S_0}{R} - \pi + \beta - \int_o^\ell\sqrt{1 + (dy/dx)^2}dx = 0 \tag{15}$$

Equations (12), (13), and (15) are the required boundary conditions. They implicitly determine three parameters: 1) the leading-edge location x_ℓ, 2) the ratio L_0/R, and 3) the angle β.

On inspecting these boundary conditions, one finds that two dimensionless parameters (in addition to α and Δ, which are given) affect the solutions. They are: 1) the ratio of the unstretched length of ballute membrane to the length of the fuselage, S_0/L_0, and 2) the quantity, to be defined as

$$\chi = \frac{L_0}{\phi}\rho U^2(1 + \Delta) \tag{16}$$

which is a measure of the ratio of internal gas pressure to elastic coefficient of the ballute membrane.

The differential equation [Eq. (7)] is integrated numerically to determine the ballute profile. A fourth-order fixed-step Runge-Kutta method was used for the intergration with integrating step dx of 0.005. The leading-edge point is reached typically at $\chi \leq 2.5$. At each integrating step, a test is made to see if Eqs. (12), (13), and (15) are satisfied simultaneously. Integration is stopped when such a point is reached. Once the geometry is found, integrations (8-11) are performed to obtain the forces and moments about the origin produced by

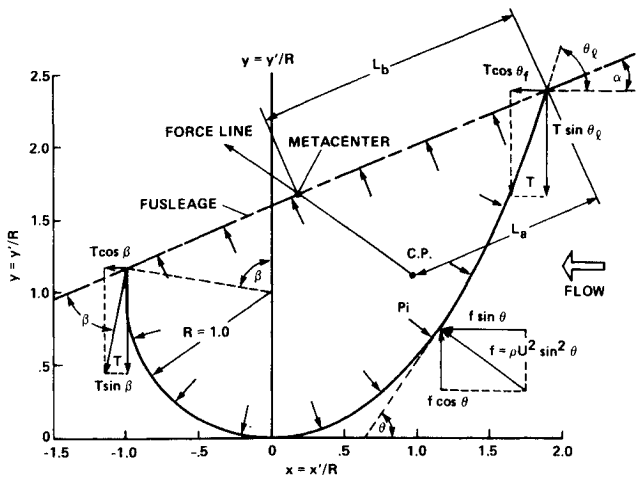

Fig. 2 Geometry and forces acting on a lower-half compartment of a two-dimensional ballute.

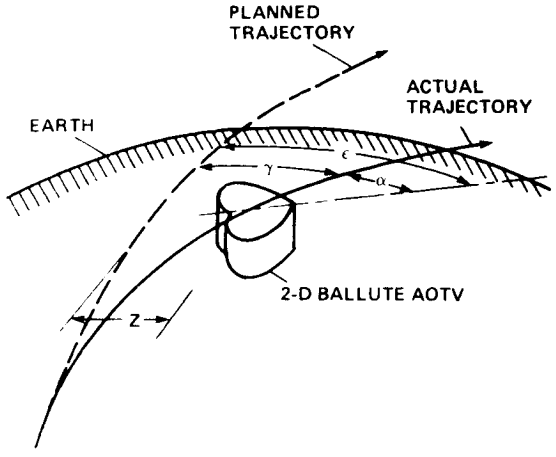

Fig. 3 Coordinate system used in calculating the trajectories of an AOTV employing a two-dimensional ballute.

one compartment. The coordinates of the c.p., x_a and y_a, are determined from

$$x_a = \text{Lift moment/lift}$$

$$y_a = \text{Drag moment/drag}$$

The moment about an arbitrary given c.g. point is then calculated using x_a, y_a, lift, drag, and the moments about the origin so obtained. The calculation is repeated for the other compartment. The forces and moment obtained for the two compartments are added to form the total forces and moment. The lift coefficient C_ℓ, drag coefficient C_d, and pitching moment coefficient C_m are then calculated from the following definitions:

$$C_\ell = \frac{\text{Lift}}{0.5\rho U^2 L_0}$$

$$C_d = \frac{\text{Drag}}{0.5\rho U^2 L_0}$$

$$C_m = \frac{\text{Total moment}}{0.5\rho U^2 L_0^2}$$

The c.p. of the two-compartment combination is then calculated by adding these forces. The distance from the leading edge to the combined c.p. is designated by L_a.

The point of interception of the force line (the vector representing the combination of the lift and drag forces) drawn from the c.p. and the body centerline has an important meaning: if the c.g. is located on the centerline ahead of this point, then the inertial force developed during atmospheric braking will produce a negative pitching moment, which tends to reduce the given angle of attack, which is a stabilizing phenomenon. Therefore, for maintaining pitching stability, this point is the farthest downstream location of c.g. that is allowed. This point closely resembles the metacenter for a marine vessel, for which the point represents the intersection between the central plane of symmetry and the vector representing the force of flotation. Therefore, this point will be referred to as the metacenter[15] and will be designated by the notation L_b. In order for a vehicle to be statically stable, therefore, the c.g. location L_c must satisfy the condition

$$L_c \leq L_b \tag{17}$$

The calculation is repeated for various values of angle of attach α, overpressure parameter Δ, the ratio of the lengths of the unstretched membrane to fuselage S_0/L_0, and the pressure-to-elasticity ratio χ. The pitching moment derivative $dC_m/d\alpha$, which must be negative in order for a vehicle to be stable, is calculated numerically from the two values of C_m corresponding to two values of α differing by 0.05 rad.

After such calculation of aerodynamic characteristics, the present work shows an example of how flight trajectories are affected by the mechanics of the ballute for a hypothetical AOTV that employs such a ballute. For this purpose, the yaw and accompanying drift motions are calculated as shown schematically in Fig. 3. The navigational bearing error (the difference between the local lateral flight-path angle and the planned trajectory lateral angle) is denoted by γ. The body angle with respect to the flight-path angle is denoted by ϵ. The lateral yaw and resulting drift motion are calculated rather than the vertical pitching motion because pitching motion causes changes in flight altitude, which is a more complicated phenomenon. A change in altitude will cause a change in χ, which, in turn, changes all aerodynamic characteristics, leading to the situation where one cannot isolate the consequence of an initial error in the body attitude angle from other effects. In calculating the vertical motion of the AOTV, lift coefficient (in the vertical direction) is assumed to be zero, as would be appropriate for a flight of a two-dimensional ballute as shown in Fig. 3. The local yaw angle of attack α is related to ϵ and γ by

$$\alpha = \epsilon - \gamma$$

The drift (the lateral deviation of the flight path) is denoted by Z. The equations governing these quantities can be written approximately as

$$I\frac{d\epsilon}{dt} = 0.5C_m\rho U^2 A L_0 \tag{18}$$

$$MU\frac{d\gamma}{dt} = 0.5C_\ell\rho U^2 A \tag{19}$$

$$\frac{dZ}{dt} = U\sin(\gamma) \tag{20}$$

where A is the area of the two-dimensional fuselage, I the moment of inertia, and M the mass of the vehicle. The values A, I, and M are based on the assumption that the fuselage is 10 m long and 5 m wide ($A = 50$ m^2), is uniform in density, and weights 5000 kg leading to $I = 5.556 \times 10^4$ kg-m^2. The last three differential equations are integrated starting from the initial conditions $\epsilon = 0.05$, $\gamma = 0$, and $Z = 0$ at the entry altitude of 150 km, simultaneously with the equations of

motion that describe the change in the flight velocity, vertical flight angle, and flight altitude. The velocity and the vertical flight angle are chosen to correspond to the case where the vehicle is returning from GEO in the equatorial plane to reach a postflight apogee of 666 km altitude when the vehicle flies with zero yaw angle of attack. The elastic constant ϕ is chosen to be 10,000 N/m, whereas S_0/L_0 is set to 1.2 for the calculation. At each point on the flight trajectory, the geometry of the ballute is determined by intergrating Eq. (7) using the local values of χ and α. The ballute solution produces C_d, C_ℓ, and C_m, which are needed in the calculation of motion of the vehicle. A sixth-order variable-step Runge-Kutta method is used for the timewise integration.

Results

Figures 4 and 5 show the ballute shapes at zero angle of attack for various values of S_0/L_0 and χ. In Fig. 4, one sees the effects of χ and S_0/L_0 on the profile for a fixed Δ. For a small χ, which results from a relatively small freestream density in comparison with the elastic coefficient of the membrane, the profile is nearly symmetric with respect to the axis that is perpendicular to the centerline. A small value of S_0/L_0 also produces a nearly symmetric profile, probably because the elongation and tension caused by the elongation are larger when S_0/L_0 is small. Figure 5 shows the effect of Δ for a fixed χ. A smaller value of Δ results from a smaller internal pressure, which causes the forebody region to sweep back because otherwise it cannot balance a high shock-layer pressure.

Figure 6 shows the variation in drag coefficient of the ballute at zero angle of attack as a function of Δ and χ. In low-density regions, $\chi = 0.01$ and 0.1, little change occurs in drag coefficient when the internal pressure is varied. Only when χ is large, does the drag coefficient vary significantly with Δ, a variation of over a factor of 5 is seen for $\chi = 1$. Therefore, in order to vary the drag coefficient during flight by inflating or deflating the ballute, one sees that χ must be maintained at an order of 1.

In Fig. 7, the shape of the vehicle at an angle of attack of $\alpha = 0.4$ rad (22.92 deg) is shown. As seen here, the windward side is depressed inward because of the increased Newtonian shock-layer pressure, while the leeside is bulging outward because of the lowered shock-layer pressure. That is, there is a significant compliance of the ballute geometry to the changes in shock-layer pressures caused by a finite angle of attack. The depression of the windward side is likely to cause a reduction in drag and increase in positive lift for the windward side, while the bulging of the leeside would cause an increase in drag and decrease in negative lift there, leading to a nose-up pitching moment, which is destabilizing. The c.p. is located at a point approximately 35% from the leading edge for this case where $L_a = 0.35L_0$. The c.p. is not on the centerline (fuselage) but is offset by a small distance $Y_a = -0.065L_0$. The metacenter is at $L_b = 0.45L_0$.

In Fig. 8, the lift coefficient C_ℓ, the pitching moment coefficient C_m, and the stability derivative $dC_m/d\alpha$ around an assumed c.g. location of $L_c/L_0 = 0.445$, and the location of the metacenter L_b/L_0 are plotted against the angle of attack. The figure shows that C_ℓ increases almost linearly with angle of attack despite the compliance of the shape with the changes in the shock-layer pressures mentioned earlier. The pitching moment C_m increases at small α's, reaching a peak at $\alpha = 0.22$ rad. As a result, $dC_m/d\alpha$ is positive up to that angle of attack and becomes negative thereafter. The angle of attack $\alpha = 0.22$ marks the boundary between the stable and unstable regions. The metacenter location L_b/L_0 is less than 0.445 at α less than 0.22 and is larger at larger α's, in correspondence with the sign of $dC_m/d\alpha$ [see Eq. (17)]. It is interesting to note that the instability is seen only at small angles of attack. If a vehicle flies at this particular condition, therefore, an oscillatory motion will continue over a small range of angles of attack but will be stable overall, as has been observed experimentally with the towed axisymmetric ballutes.[8-10]

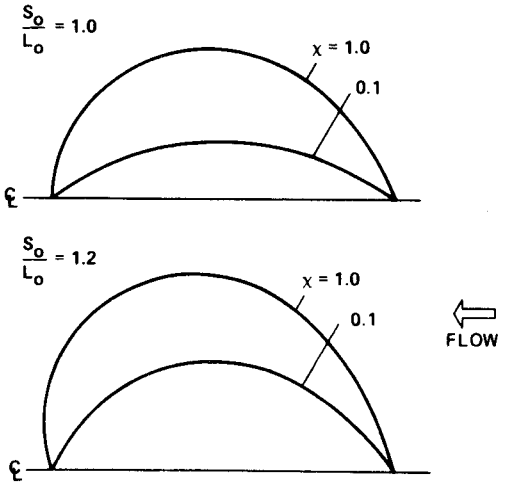

Fig. 4 Typical ballute upper-half profiles at $\alpha = 0$ and $\Delta = 0.5$.

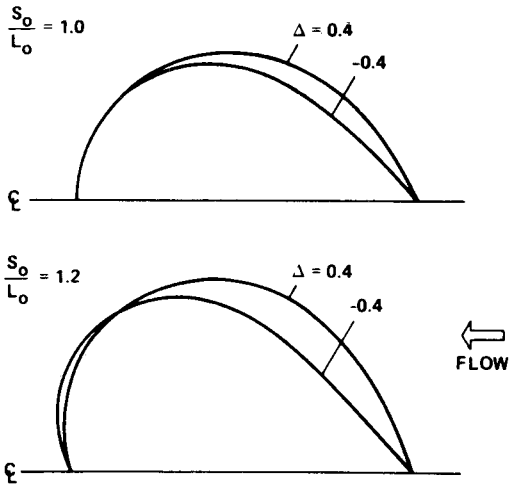

Fig. 5 Typical ballute upper-half profiles at $\alpha = 0$ and $\chi = 1$.

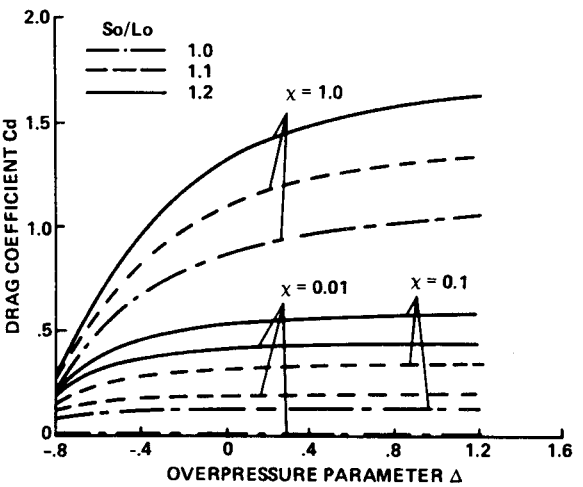

Fig. 6 Variation of C_d as a function of Δ and χ at $\alpha = 0$.

It must be noted here that there is a limit to the angle of attack for which a solution is possible. At angles of attack greater than a certain critical value, usually above 0.7 rad, the solution of Eq. (7) satisfying the constraint equations (12), (13), and (15) cannot be found. Mathematically, at the critical

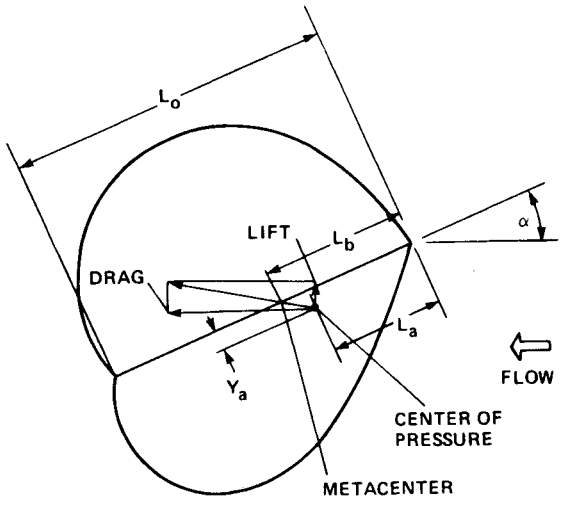

Fig. 7 Ballute geometry for $\chi = 1$, $S_0/L_0 = 1.2$, $\Delta = 0$, and $\alpha = 0.4$.

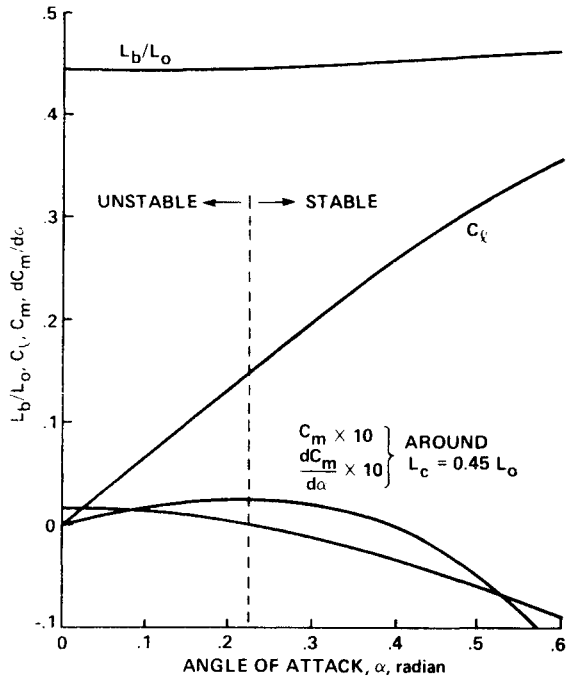

Fig. 8 Variation of C_ℓ, L_b/L_0, C_m, and $dC_m/d\alpha$ for $\Delta = 0$, $S_0/L_0 = 1.2$, and $L_c/L_0 = 0.445$.

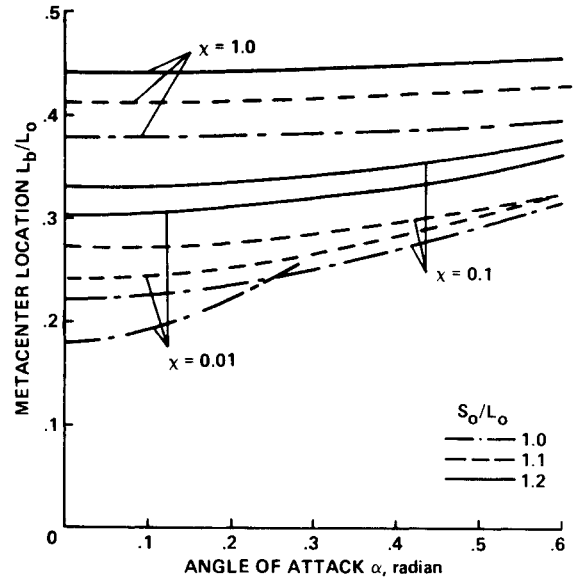

Fig. 9 Variation of L_b/L_0 as a function of α, S_0/L_0, and χ for $\Delta = 0$.

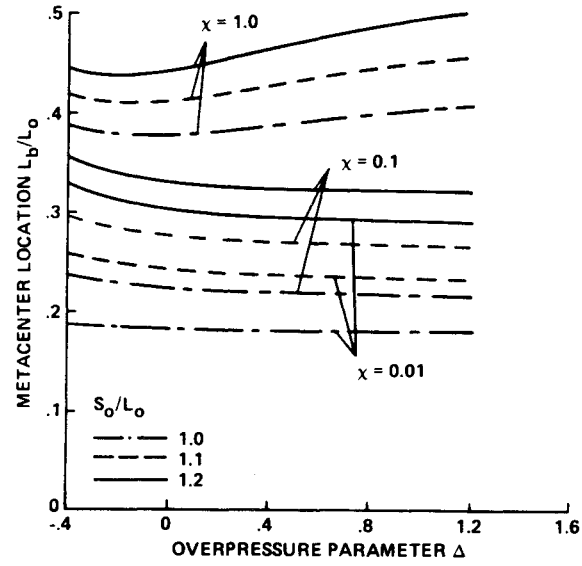

Fig. 10 Variation of L_b/L_0 as a function of Δ, S_0/L_0, and χ for $\alpha = 0$.

angle of attack, a zero curvature occurs on the membrane surface. Physically, this must mean that the shape of the ballute begins to collapse at such a large angle of attack.

In Fig. 9, the location of the metacenter is shown as a function of α, S_0/L_0, and χ for a fixed Δ value of 0. As seen here, the metacenter is within the forward half of the vehicle length: $L_b/L_0 \leq 0.46$. At $\chi = 1.0$, it is between 0.38 and 0.46. For smaller χ values, however, the metacenter is fairly small, reaching as low as 0.18 for $\chi = 0.01$. This means that the ballute tends to be unstable at high altitudes where the density is small. For the same χ value, a larger S_0/L_0 yields higher stability. For cases where there is an overlap and crossover for $\chi = 0.1$ and 0.01, a hysteresis may occur in stability in certain low-density regions. One notes here that the L_b values for the ballute are considerably smaller than the typical L_b values are for a rigid body. In Ref. 14, the metacenter is determined for sphere cones of half-cone angles in the range of 40–80 deg. For the same cone angle and body radius, the two-dimensional ballute under consideration has a considerably smaller L_b value than does the sphere cone. One could attribute this difference to the compliance of the ballute membrane with the changes in shock-layer pressures.

In Fig. 10, the metacenter location is shown as a function of Δ, S_0/L_0, and χ. One sees here that the metacenter is relatively insensitive to the Δ value. Smaller χ values lead consistently to smaller L_b values, and no crossover phenomenon is seen in this plot.

Figure 11 shows the results of the trajectory calculations. The initial entry conditions correspond to those for a mission in which an AOTV returns from the GEO flying within an equatorial plane, to attain a postflight apogee altitude of 666 km. The yawing and accompanying drift motions are calculated as shown schematically in Fig. 3. The yaw angle is assumed to be 0.05 rad at the time of entry, $t = 0$. The calculation thus tests the consequences of a small initial error in angle of attack on subsequent motions of the vehicle. The remaining environmental parameters for this calculation were given in the section entitled "Method of Calculation." The top part of Fig. 11 shows the changes in altitude and in χ for three different values of L_c/L_0. As seen in the figure, the perigee point is at an altitude of approximately 77 km for this

case. The quantity χ takes the maximum value of approximately 2 at the perigee. Both the cases of L_c/L_0 of 0.3 and 0.4375 complete the atmospheric flight successfully, but their trajectories are slightly different. Although not shown, the postflight apogee altitude for the 0.4375 case was found to be 268 km lower than the 0.3 case. The case of $L_c/L_0 = 0.4438$ fails at $t = 105$ s, because of the divergence of the angle of attack visualized in the middle portion of the figure.

In the middle portion of Fig. 11, the case of 0.3 shows a monotonic decrease of the angle of attack from the initial given value of 0.05 rad toward zero. The 0.4375 case shows an initial increase in the angle of attack, reaching a peak at approximately 95 s and subsequently subsiding to zero. The initial increase is due to the unstable moment, which is caused at the low densities mentioned earlier. Fortunately for this case, a stable moment is produced by the higher densities (Fig. 8), beginning at approximately $t = 95$ s, to restore the angle of attack to zero in time. For the case of $L_c/L_0 = 0.4438$, however, the angle of attack increases to a value that causes the ballute to collapse before reaching the stable high-density region. The vehicle thus tumbles at around $t = 105$ s. The lower part of Fig. 11 shows the lateral drift of the ballute. The case of $L_c/L_0 = 0.4375$ shows a drift of approximately 13 km at $t = 600$ s. The 0.4375 case should be considered to be marginally acceptable for successful atmospheric flight.

Discussion

First, the calculated results show that the drag coefficient of a two-dimensional ballute can be varied over a large range by varying the internal pressure: A factor of 5 change in drag coefficient is possible when χ is unity (Fig. 6). It seems, therefore, that an elastic ballute can be an effective device for modulation of drag for use as an aerobrake for an AOTV, as suggested in Refs. 3 and 5.

The problem of a ballute resides mainly with the difficulty concerning aerodynamic stability. The present work shows that the c.p. and the metacenter of a two-dimensional ballute are located relatively close to the leading edge and, hence, for the vehicle to be stable the c.g. must also be placed near the leading edge. This feature is believed to be caused by the compliance of the elastic membrane in response to the aerodynamic forces. As mentioned earlier, at a finite angle of attack, the windward side surface is depressed inward and the leeside surface bulges outward because of the changes in the shock-layer pressures (Fig. 7). The result is that more lift and less drag are produced by the windward side, whereas less lift and more drag are produced by the leeside, all of which contribute to the destabilizing moment. In order to be stable at all freestream densities, the c.g. must be within the forward 18% of the length of the vehicle. Placing the c.g. so close to the leading edge is impractical and almost certainly unachievable for a realistic AOTV. This difficulty is relaxed somewhat by the fact that the duration over which the AOTV flies through the destabilizing low-density region is limited; as Fig. 11 shows, a vehicle with the c.g. at the 43.75% point can survive the flight without tumbling. Thus, one finds that there is a range, between 18 and 43% in this case, which, if the c.g. is placed within it, leads to conditional stability.

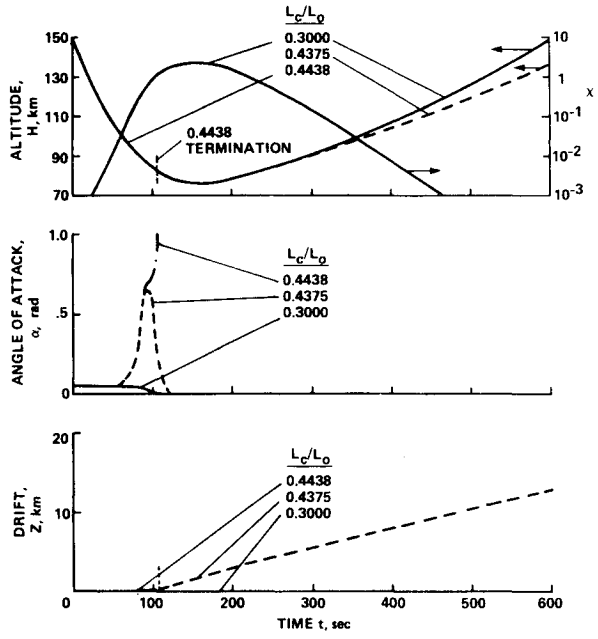

Fig. 11 Variation in altitude, χ, α, and Z as a function of time t for three different L_c/L_0 values; for $\Delta = 0$, $S_0/L_0 = 1.2$, $\phi = 10{,}000$ kg/m, for an AOTV returning from GEO in the equatorial plane.

However, placing the c.g. within the forward 43.75% at all times may still be difficult to realize. For instance, if the fuel tanks are placed in the forward position and are empty while the payload is placed at the rear position, as has been proposed (see Refs. 2 and 15), then the c.g. will be close to the rear end of the vehicle. Even if the c.g. could be maintained at the 43.75% point, the vehicle's stability cannot be guaranteed. At high altitudes, where the AOTV's are expected to fly, a large spatial nonuniformity in density is known to occur.[16] If the vehicle encounters such a low-density region, the ballute will develop a destabilizing moment. Thus, there is a risk in placing the c.g. so close to the aft end of the conditionally stable c.g. range.

The present finding about the limits of allowed c.g. should at least be qualitatively applicable to the case of an axisymmetric body. For an axisymmetric ballute, the pitching moment is produced mostly by the part of the ballute membrane surface that is far from the centerline, which resembles the two-dimensional ballute considered in the present work. The compliance phenomenon seen for the two-dimensional ballute will occur also for the axisymmetric ballute, which leads to a similar result.

The present analysis identifies three parameters – the ratio of the internal gas pressure to the total pressure of the freestream $(1 + \Delta)$, the ratio of the length of unstretched membrane to the length of the vehicle S_0/L_0, and the ratio of the product of the inside gas pressure and vehicle length to the elastic coefficient of the membrane χ – to be the controlling parameters of the problem. If one wishes to conduct a subscale experiment in a laboratory, these parameters must be reproduced in order to obtain the correct stability characteristics. Since χ is proportional to the length of the vehicle and, therefore, is scale dependent, care must be taken to match this parameter.

Conclusions

Idealized two-dimensional ballutes proposed for aeroassisted orbital transfer vehicles (AOTV's) show promise of being able to modulate drag over a large range. However, difficulty exists in that center of pressure and the allowed limit of center of gravity (metacenter) are located close to the leading edge, especially when the freestream density is low. This phenomenon is believed to be due to the compliance of the elastic membrane of the ballute in response to the changes in shock-layer pressures that are caused by the changes in angle of attack. In order for the ballute to be stable at all freestream densities, the center of gravity must be located within the forward 18% of the length of the vehicle. However, if the trajectory of an AOTV can be tailored so that it passes through the unstable low-density regime quickly, then the center of gravity may be placed as far aft as 43.75%.

References

[1]Walberg, G. D., "Survey of Aeroassisted Orbit Transfer," *Journal of Spacecraft and Rockets*, Vol. 22, Jan.-Feb. 1985, pp. 3-18.

[2]Park, C., "A Review of Shock Waves Around Aeroassisted Orbital Transfer Vehicles," NASA TM-86769, June 1985.
[3]Andrews, D. G. and Bloetscher, F., "Aerobraked Orbital Transfer Vehicle Definition," AIAA Paper 81-0279, Jan. 1981.
[4]Grenich, A. F. and Woods, W. C., "Flow Field Investigation of Atmospheric Braking for High Drag Vehicles with Forward Facing Jets," AIAA Paper 81-0293, Jan. 1981.
[5]Andrews, D. G., Caluori, V. A., and Bloetscher, F., "Optimization of Aerobraked Orbital Transfer Vehicles," AIAA Paper 81-1126, June 1981.
[6]Lauers, J. K., "The Ballute–A Retardation Device and Wind Sensor," Dayton Univ. Research Inst., Dayton, OH, TR UDRI-TR-67-144, Nov. 1967.
[7]Barton, R. R., "Development of Attached Inflatable Decelerators for Supersonic Application," NASA CR-66613, May 1968.
[8]Mayhue, R. J. and Eckstrom, C. V., "Flight-Test Results from Supersonic Deployment of an 18-Foot-Diameter (5.49-Meter) Towed Ballute Decelerator," NASA TM X-1773, May 1969.
[9]Usry, J. W., "Performance of a Towed, 48-Inch-Diameter (121.92-cm) Ballute Decelerator Tested in Free Flight at Mach Numbers from 4.2 to 0.4," NASA TN D-4943, Feb. 1969.
[10]Reichenau, D. E. A., "Deployment and Performance Characteristics of Attached Inflatable Decelerators with Mechanically Deployed Inlets at Mach Numbers from 2.6 to 4.5," Arnold Engineering Development Center, Arnold Air Force Station, TN, TR AEDC-TR-72-90, June 1970.
[11]Aebischer, A. C. and Suters, E. S., Jr., "Development Status of Ballute System for Stabilization and Retardation of Aircraft Stores," AIAA Paper 70-1200, Sept. 1970.
[12]McGirr, P. G., Aebischer, A. C., and Weinberg, S. A., "Development and Testing of Ballute Stabilizer/Decelerators for Aircraft Delivery of a 500-lb Munition," AIAA Paper 73-485, May 1973.
[13]Pyle, J. S., Phelps, J. R., and Baron, R. S., "Performance of a Ballute Decelerator Towed Behind a Jet Airplane," NASA TM X-56019, Dec. 1973.
[14]Weilmuenster, K. J. and Hamilton, H. H. II, "A Comparison of Computed and Measured Aerodynamic Characteristics of a Proposed Aeroassist Flight Experiment Configuration," AIAA Paper 86-1366, June 1986.
[15]Davies, C. G. and Park, C., "Aerodynamics of Generalized Bent Biconics for Aero-Assisted, Orbital-Transfer Vehicles," *Journal of Spacecraft and Rockets*, Vol. 22, March-April 1985, pp. 104–111.
[16]Blanchard, G. P. and Buck, G. M., "Determination of Rarefied-Flow Aerodynamics of the Shuttle Orbiter from Flight Measurements on STS-6 and STS-7," AIAA Paper 85-0347, Jan. 1985.